

Early detection of faults in DC motors extends their life and lowers their power usage. There are a variety of traditional and soft computing techniques for detecting faults in DC motors. Many diagnostic techniques have been developed in the past to detect such fault-related patterns. These methods for detecting the aforementioned potential failures of motors can be utilized in a variety of scientific and technological domains. Motor Power Pattern Analysis (MPPA) is a technology that analyzes the current and voltage provided to an electric motor using particular patterns and protocols to assess the operational status of the motors without disrupting production. Engineers and researchers, particularly in industries, face a difficult challenge in monitoring spinning types of equipment. In this work, we are going to explain how to use the motor power pattern/signature analysis (MPPA) of a power signal driving a servo to find mechanical defects in a gear train. A hardware setup is used to simplify the demonstration of obtaining spectral metrics from the power consumption signals. A DC motor, a set of metal or nylon drive gears, and a control circuit are employed. The speed control circuit was eliminated to allow direct monitoring of the DC motor's current profiles. Infrared (IR) photo-interrupters with a 35 mm diameter, eight-holed, standard servo wheel were employed to gather the tachometer signal at the servo's output. The mean value of the measurements was 318 V for the healthy profile, while it was 330 V for the faulty gears power data. The proposed power consumption profile analysis approach succeeds to recognize the mechanical faults in the gear-box of a DC servomotor via examining the mean level of the power consumption pattern as well as the extraction of the Power Spectral Density (PSD) through comparing faulty and healthy profiles

Keywords: monitoring, DC servomotor, power consumption, pattern recognition, power profile, mechanical faults

Received date 28.06.2021

Accepted date 25.08.2021

Published date 29.10.2021

How to Cite: Majdi, H. S., Shijer, S. S., Abduljabbar, O. H., Habeeb, L. J., Sabry, A. H. (2021). Analysis of fault diagnosis of dc motors by power consumption pattern recognition. *Eastern-European Journal of Enterprise Technologies*, 5 (5 (113)), 14–20. doi: <https://doi.org/10.15587/1729-4061.2021.240262>

1. Introduction

The condition monitoring of direct current (DC) motor is essential for early warning of potential failures in machines and industrial applications. Engineers and academics, particularly in industries, have found monitoring a spinning machine to be a difficult undertaking. Vibration analysis is a useful tool for determining the current machine state, detecting problems of inoperative equipment, and monitoring overall machine health. Exact vibration determination, bearing condition determination and Fast Fourier Transform (FFT) analysis are the three components of full vibration analysis [1, 2].

The reasons for faults can be classified into two clusters:

1) Failures due to mechanical causes that include mechanical unbalance, misalignment, end rings or fractured rotor bars, bearing fatigue, loss of cooling, improper lubrication, overheating;

ANALYSIS OF FAULT DIAGNOSIS OF DC MOTORS BY POWER CONSUMPTION PATTERN RECOGNITION

Hasan Shakir Majdi

Dean

Department of Chemical Engineering and Petroleum Industries
Al-Mustaqbal University College
Hillah, Babil, Iraq

Sameera Sadey Shijer

Lecturer Doctor*

Abduljabbar Owaid Hanfesh

Assistant Professor Doctor

Department of Electromechanical Engineering**

Laith Jaafer Habeeb

Assistant Professor Doctor*

Ahmad H. Sabry

Corresponding author

Doctor of Control and Automation Engineering

Department of Institute of Sustainable Energy

Universiti Tenaga Nasional

Jalan Ikram-Uniten, Kajang, Selangor, Malaysia, 43000

E-mail: ahs4771384@gmail.com

*Training and Workshop Center**

**University of Technology

Baghdad, Iraq

2) Failures due to electrical causes that include impedance and resistance unbalancing, poor power quality, insulation breakdown, and excessive current and loading. The distribution of DC motor major faults can be listed as bearing (69 %), stator winding (21 %), rotor bar (7 %), and shaft/coupling (3 %) faults [3].

Motor Power Pattern Analysis (MPPA) is a technology that analyzes the current and voltage provided to an electric motor using particular patterns and protocols to identify the operational state of the motor without disrupting production. Machine diagnostic choices are made using MPPA, as well as vibration and temperature analysis. MPPA is based on the idea that an induction motor circuit functions as a transducer. Variations in motor current can be noticed by clamping a Hall-Effect current sensor on either the primary or secondary circuit.

Many diagnostic techniques have been developed in the past to detect such fault-related patterns. These methods for detecting the aforementioned potential failures of mo-

tors could utilize a variety of scientific and technological domains. According to the studies [4–7], it is possible to classify the fault diagnosis as depicted in Fig. 1.

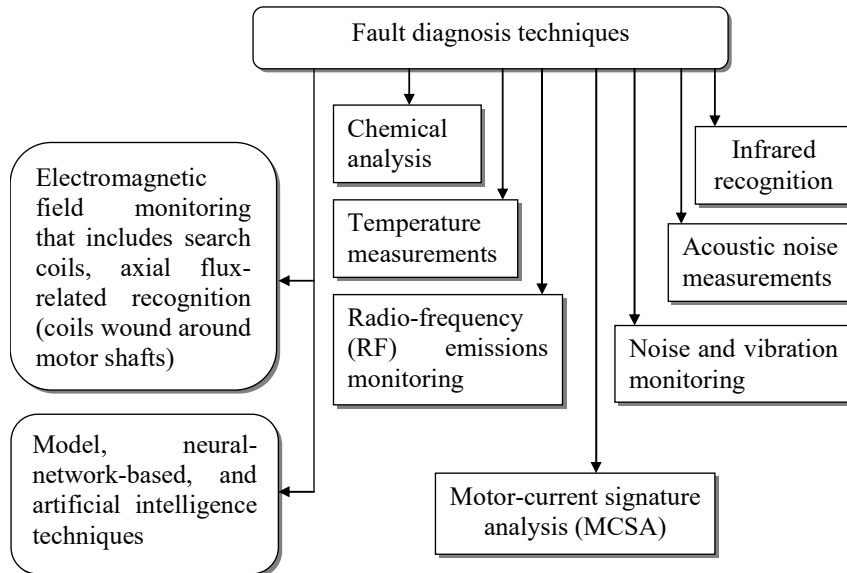


Fig. 1. Fault diagnosis techniques

Therefore, noninvasive motor-current signature analysis is by far the most popular technique for diagnosing problems, according to diverse research. However, to separate the significant frequency components from others that may be present due to time harmonics, machine saturation, or mechanical difficulties, modeling and measurement-driven methods of machine defects are required.

2. Literature review and problem statement

Several studies discussed fault detection and diagnosis by analyzing the current or power consumption signatures/patterns. The paper [8] analyzed the motor model parameters like torque (τm), speed (ω), and motor current (I) to the back electromotive force (EMF) (e) relationships for a DC servomotor dynamic model. This study provides useful information on the electrical components (resistance (R_a) and armature inductance (L_a)) and the mechanical components (viscous friction and damping, and shaft inertia). However, there were unresolved issues related to the information describing the potential faults on DC motors individually, it reported an analysis for a robotic system including 6 DC motors instead. The study [3] adopted three methods (recurrent networks, support vector machine, and convolutional networks) to handle the challenges of Fault Detection and Isolation (FDI) of incipient errors of a DC motor. Although the experimental results of the study revealed that the convolutional networks achieve a better diagnosis, the study didn't discuss the model parameters like torque (τm), speed (ω), motor current (I), and the back electromotive force (EMF) (e) relationships. The authors in [9] developed a statistical-based model for fault diagnosis to detect motor windings short-circuit faults and provide also an estimation for a fault severity. This work estimated fault severities to make proper decisions in reaction to the fault conditions. However, the study lacked from proving a mathematical model with experiments. The paper [10] presented a method based on the characteristics of acquired

Hall-vector stages and through a Clark-vector transformation of the Hall signal to identify Hall fault type by detecting their phase change of a motor. The work investigated the impact of various faults on the accuracy of rotor position estimations, and two fault-tolerant management techniques were proposed. However, this study discussed only two faults on AC induction motor.

In the work [11], the fault diagnosis unit was set up to gather fault data. A residual matching technique is used to find the problem when the actuator defect is identified by comparing the residual signal to a predetermined threshold. A least-squares filter can be used to further estimate deflection processes. A fault-tolerant controller was designed based on the fault estimation to ensure the DC motor system's stability and control performance. However, this method is too complicated and time-consuming when implemented.

The study [12] presented a fault diagnosis for a DC motor via thermal pattern instead of current recognition using experiments employing a data logger with a K-type thermocouple. Although temperature measurements were performed on 4 parts of a DC motor including casing, brush, bearing, and permanent magnet, the dependency on thermal measurements is not sufficient to predict all potential faults of DC motors. A way to overcome these difficulties can be another technique for fault diagnosis, which is proposed by [13], where wavelet examination with starting transient current was used to quantify and classify the bearing and armature winding faults in a DC motor. However, this work investigated only two types of faults, while leaving other potential failures. All this suggests that it is advisable to conduct a study on building a platform for mechanical fault diagnosis of DC motors through power consumption pattern recognition.

3. The aim and the objectives of the study

The study aims to build a platform for mechanical fault diagnosis of DC motors through power consumption pattern recognition.

To achieve this aim, the following objectives are accomplished:

- to recognize the mechanical faults in the gear-box of a DC servomotor via the power consumption pattern and its mean value;
- to identify frequencies of interest by computing nominal RPM;
- to extract data of Power Spectral Density (PSD) after constructing the band of frequency that may contain fault indication.

4. Materials and methods

4.1. DC servomotor mathematical model

The manufacturers provide some of the initial physical parameters, such as motor torque T , armature current i , and constant factor (K_t), as follows [1, 2]:

$$T = K_t \cdot i.$$

The back-EMF (e) is proportional to the angular velocity of the shaft ω by a constant factor (K_e):

$$e = K_e \cdot \omega.$$

In SI units, the motor torque and back-EMF constants are equal, that is,

$$K = K_t = K_e.$$

The system is modeled by summing the torques that act on the rotor inertia and integrate the angular acceleration of the rotor to provide the velocity and integrate the velocity to obtain the position. Kirchhoff's laws are also applied to the armature circuit. First, a modeling of the integrals of the rotor acceleration and the rate change of armature current is calculated [3, 4], as follows:

$$\frac{d^2\theta}{dt^2} dt = \int \frac{d\theta}{dt} dt = \theta,$$

$$\int \frac{di}{dt} dt = i.$$

Next, Newton's and Kirchhoff's laws are applied to the motor system to generate the following equations:

$$J \frac{d^2\theta}{dt^2} = T - b \frac{d\theta}{dt} \Rightarrow \frac{d^2\theta}{dt^2} = \frac{1}{J} \left(K_t i - b \frac{d\theta}{dt} \right),$$

$$L \frac{di}{dt} = -Ri + V - e \Rightarrow \frac{di}{dt} = \frac{1}{L} \left(-Ri + V - K_b \frac{d\theta}{dt} \right).$$

4. 2. Experimental setup

In this work, we are going to explain how to use the motor power pattern/signature analysis (MPPA) of a power signal driving a servo to find mechanical defects in a gear train. MPPA is proven as a method for diagnosing flaws that produce torque or speed fluctuations in motor fault investigation. It is difficult to detect mechanical gear faults with typical vibration instruments, especially when the gear train isn't conveniently accessible for instrumentation with accelerometers or other vibration sensors. This method demonstrates how to use current-voltage signature analysis to derive spectral metrics to detect problems in servomotor drive gears. The hardware setup to simplify the demonstration of obtaining spectral metrics from the power consumption signals is shown in Fig. 2.

A typical Futaba-S3003 servomotor was modified for continuous rotary motion, and the electrical current data was received from it. Servos translate the internal DC motor's high speed to high torque at the output. A DC motor, a set of metal or nylon drive gears, and a control circuit are employed. The speed control circuit was eliminated to allow direct monitoring of the DC motor's current profiles. Infrared (IR) photo-interrupters with a 35 mm diameter, eight-holed, standard servo wheel were employed to gather the tachometer signal at the servo's output.

The DC servomotor was set to constant 5 V, and the output shaft speed was roughly 50 RPM due to four pairs of gears that supplied a 278:1 speed reduction. By monitoring the voltage drop across a 0.5 Ohm resistor, the current consumption was determined using Ohm's law. The current data

was amplified using a single-supply sensor interface amplifier since the change in current measurement values was too small to observe. The amplified current signals were then noise-free and smoothed using a 5th order elliptic low-pass filter (LPF) or Bode-equations vector-fitting (BEVF) filter [14] before being sent to an Arduino microcontroller via an ADC converter.

As seen in Fig. 3, the Futaba-S3003 servomotor is made up of four pairs of gears.

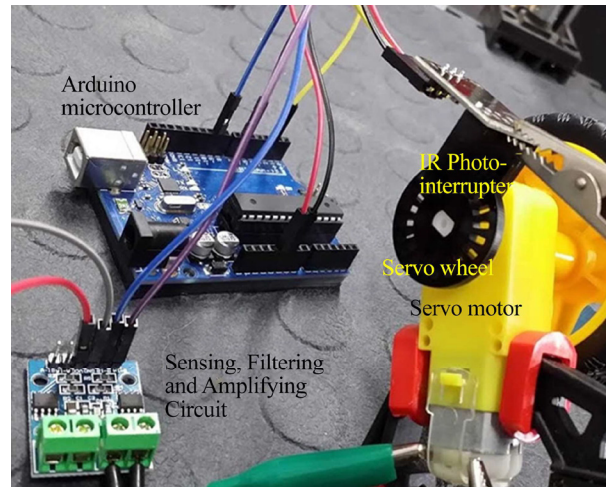


Fig. 2. Experimental setup

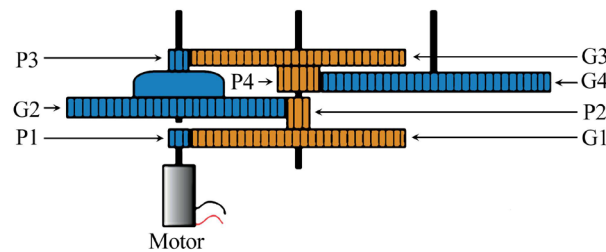


Fig. 3. Futaba-S3003 servomotor

The stepped gear G1 meshes with the pinion P1 on the motor shaft. The pinion P2, which meshes with the stepped gear G2, is a cast component of the stepped gear G1. The stepped gear G3 meshes with the pinion P3, which is a cast component of the gear G2. The pinion P4, which is cast with G3, meshes with the output gear-spline attached final gear G4. G1 and P2, G2 and P3, and G3 and P4 are free spinning gear sets, meaning they are not connected to their respective shafts. When the motor is operated at 5 volts, the set of drive gears reduces the motor speed from 13901 RPM at around 50 RPM at the output.

Before the defects in the stepped gears, G2 and G3 are applied, a total of 10 healthy data sets are acquired. Because the gears are made of nylon, they are given simulated fractures by cutting holes in the tooth spacing using a normal knife. The tooth spacing is the distance between every two consecutive teeth measured around the spur gear's pitch circle. The depths of the slots were around 70 % of the gear radius. After the defects in the gears, G2 and G3 were applied, a total of 10 incorrect data sets were collected.

Constructing frequency bands is a necessary step in calculating spectral metrics. First, we calculate the frequencies of interest using the tooth count of the drive gears in the gear train and the nominal RPM. The methodology diagram can be represented as shown in Fig. 4.

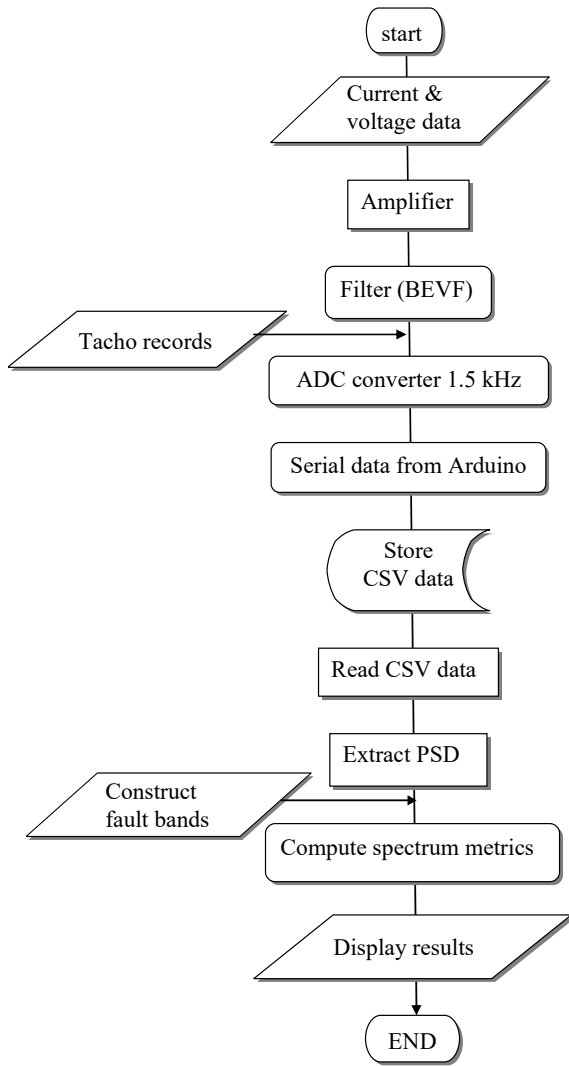


Fig. 4. Methodology diagram

As illustrated in the flowchart, the current signal is first boosted and filtered with an amplifier and a filter. The ADC of the Arduino microcontroller is used to record the current measurements at 1.5 kHz, together with tachometer pulses, to a PC as serial data at 115200 baud-rate. A MATLAB-based code is used to obtain serial data from the Arduino microcontroller to write and save to a CSV file. The CSV file is processed and read to get the spectrum metrics.

A 10×2 table is obtained with each timetable corresponding to one dataset. The 1st column of this table consists of 10 healthy data, whereas the 2nd column consists of 10 faulty data timetables, and each dataset comprises about 11 seconds of 1.5 kHz sampled data.

5. Results of the proposed approach

5.1. Results of power consumption profile recognition

The tachometer signal is in the 1st column of each generated 10×2 table, while the power consumption data is in the 2nd column that can be visualized with the tachometer pulses over time in Fig. 5.

The power consumption profile of healthy and faulty data shows a significant difference in the pattern mean level and shape.

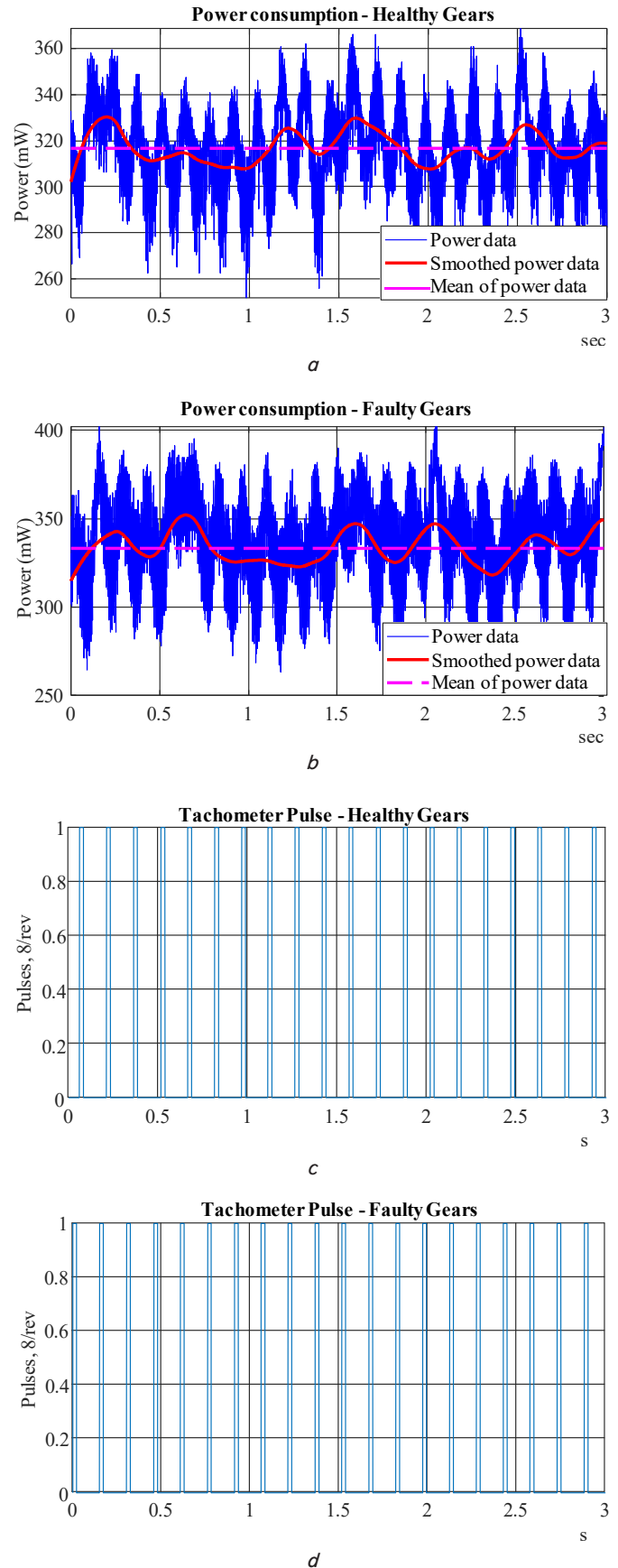


Fig. 5. Time-based profile measurements of: *a* – healthy gears power consumption; *b* – faulty gears power consumption; *c* – healthy gears tachometer pulse; *d* – faulty gears tachometer pulse

5. 2. Results of Computing Nominal RPM

In order to identify frequencies of interest, we calculated the nominal speed of the gear-box to appropriately match them with the power spectrum frequencies that are more demonstrated by visualizing the tachometer RPM records at the 1.5 kHz sampling frequency, for the healthy tachom-

eters as shown in Fig. 6 whereas these results for the faulty tachometer are shown in Fig. 7.

It's worth noting that the speed of the output shaft of the healthy and faulty data sets differs just a little. The theoretical value of 50 RPM is also close to the actual nominal RPM value.

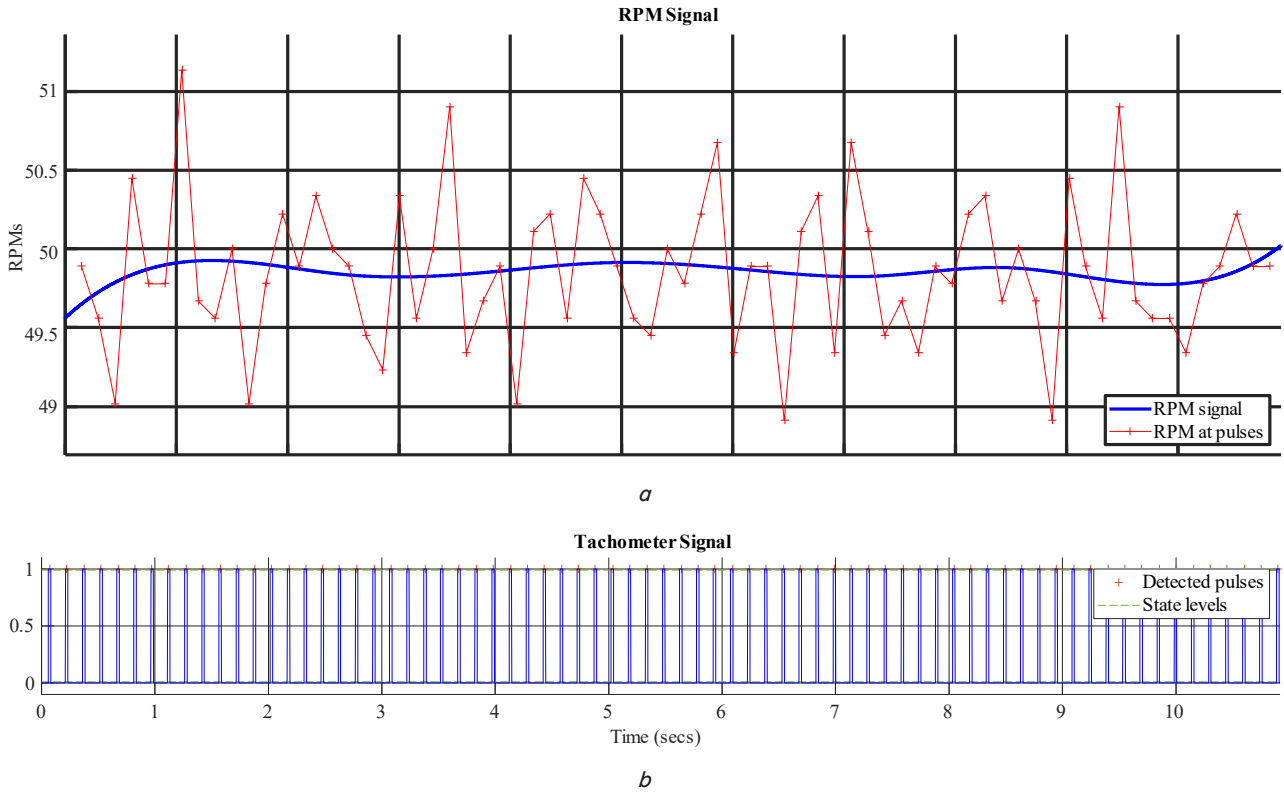


Fig. 6. Healthy results of: *a* – computing the nominal speed at the gear-box; *b* – tachometer RPM records

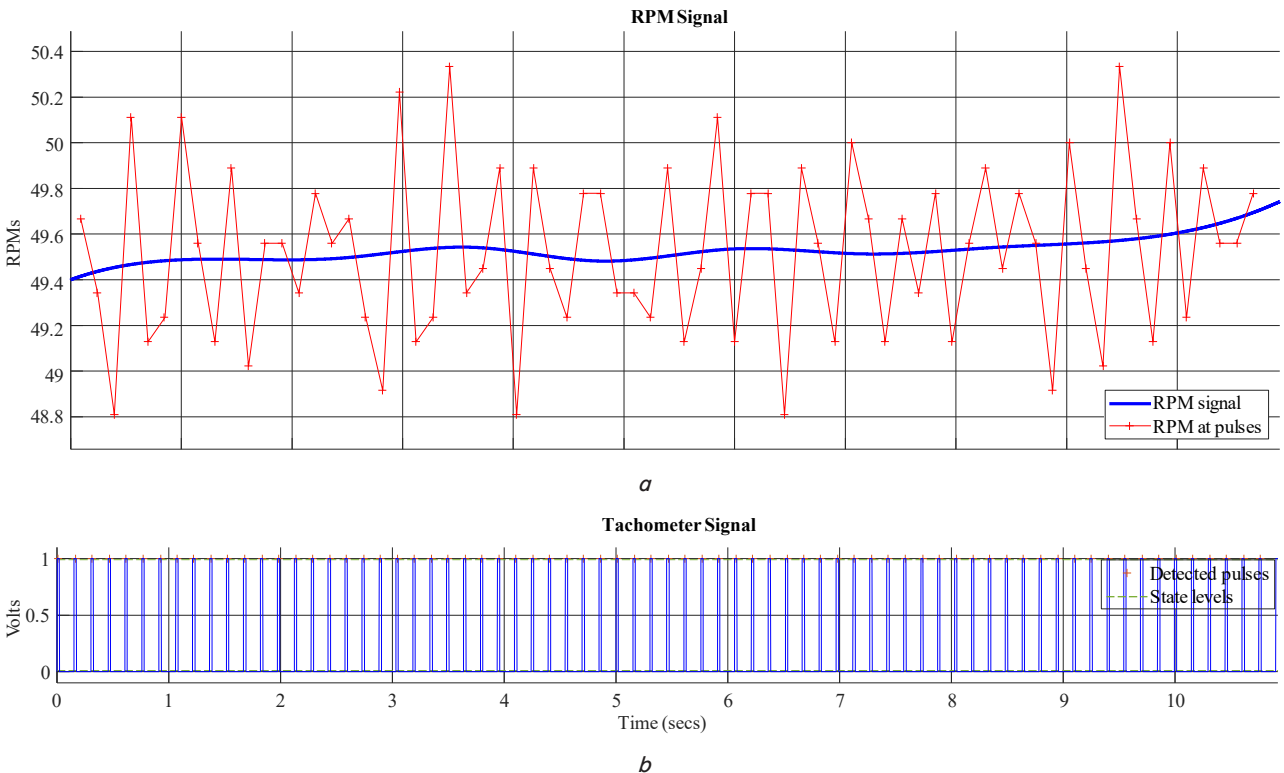


Fig. 7. Faulty results of: *a* – computing the nominal speed at the gear-box; *b* – tachometer RPM records

As a result, for both the healthy and faulty signal analysis, we used the same value of 49.9 RPM.

5.3. Results of extracting Power Spectral Density (PSD)

The actual output speed values in Hz that are close to the theoretical values are the frequencies of interest. These values including the teeth count, potential output speed, gear mesh frequencies, and cumulative gear reduction at each gear mesh are listed in Table 1 below.

Then, using Matlab’s function called “faultBands”, we created frequency bands for all of the output speeds, which included the following frequencies of interest:

- f_{S1} at 231.7 Hz, 0:1 sidebands of f_{S2} , with the 1st two-harmonics;
- f_{S2} at 37.4 Hz, 0:1 sidebands of f_{S3} , with the 1st two-harmonics;
- f_{S3} at 7.47 Hz with the 1st two-harmonics;
- f_{S4} at 2.14 Hz with the 1st two-harmonics.

Here, we calculated and displayed the faulty and healthy data’s power spectrum. The drawing of the interested frequencies on the spectrum plot is shown in Fig. 8.

The blue plot represents the healthy data spectrum, whereas the red plot represents the faulty data spectrum. By observing the increase in fault frequency amplitudes in the graph, the following points can be remarked: $1f_{S1}$ at 231.7 Hz, the corresponding sidebands, and its 2nd harmonic $2f_{S1}$ at 463 Hz.

The remaining frequencies were obtained by zooming in from 0–100 Hz as shown in Fig. 9.

Fig. 9 shows the rise in amplitudes at the frequencies:

- $1f_{S2}$ at 37.3 Hz and its corresponding sidebands;
- $1f_{S3}$ at 7.47 Hz and its 2nd harmonic $2f_{S3}$ at 14.9 Hz;
- $1f_{S4}$ at 2.14 Hz and its 2nd harmonic $2f_{S4}$ at 4.2 Hz.

Fig. 9 also shows how the faulty and healthy patterns or datasets are shifted in different levels of the power spectrum plot. As a result, by examining the power consumption pattern of a servomotor, we can categorize faulty and healthy signals.

Theoretical values calculated from tooth count assuming 50 RPM at the output shaft

Pin-ion	Gear	Pinion Teeth	Gear Teeth	Output Speed		Gear Mesh Frequency (Hz)	Cumulative Gear Reduction
				(RPM)	(Hz)		
P1	No	10	Nt	13901.6	231.69	Nm	1
P2	G1	10	62	2242.2	37.37	2316.9	6.2
P3	G2	10	50	448.5	7.47	373.7	31
P4	G3	16	35	128.1	2.14	74.7	108.5
No	G4	Np	41	50	0.83	34.2	278

Note: No, Nt, Np, and Nm refer to non-corresponding (gear, pinion teeth, gear mesh frequency), respectively.

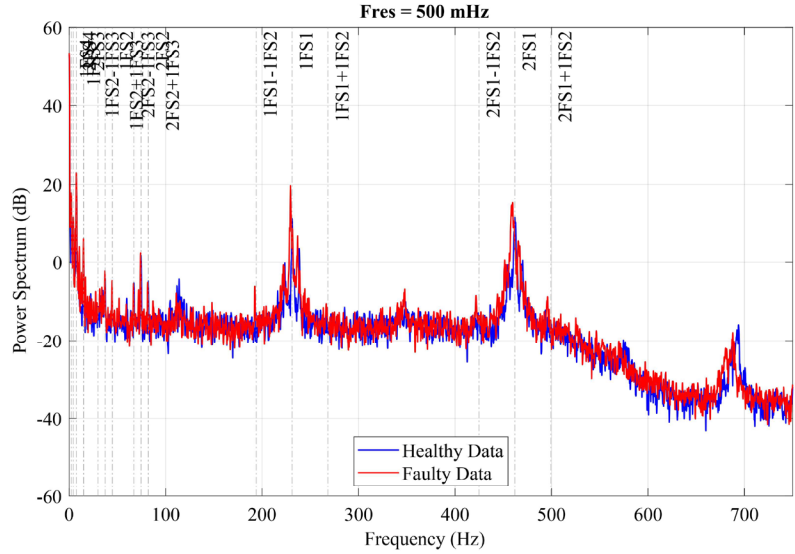


Fig. 8. Power spectrum of healthy and faulty data

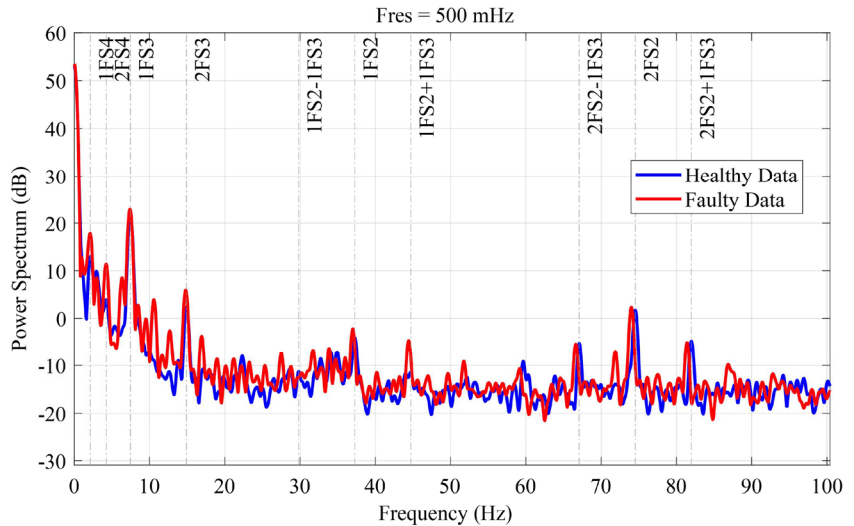


Fig. 9. (0–100) Hz zoom Power spectrum of healthy and faulty data

6. Discussion of the study results of power consumption pattern recognition

From analyzing the results of power consumption, shown in Fig. 5, it is observed that the power consumption profile of healthy and faulty data shows a significant difference in their pattern mean levels and shapes.

The mean of the power consumption measurements on the healthy gears operation was 318 V, while the mean value of the faulty gears power consumption measurements was 330 V. Furthermore, the power consumption profile of healthy and faulty data shows a significant difference in the pattern mean level and shape.

Referring to the results shown in Fig. 6, 7, there is just a little difference in computing the Nominal RPM between the speed of the output shaft at the healthy and faulty dataset conditions. In addition, the theoretical value was 50 RPM, which is also close to the actual nominal RPM value. Therefore, we perform more analysis to verify the difference.

Table 1

The result of extracting Power Spectral Density (PSD) shown in Fig. 8,9 is obtained after getting the data of constructing frequency bands. The PSD profiles show how the faulty and healthy patterns or datasets are shifted in different levels of the power spectrum plot. As a result, by examining the power consumption pattern of a servomotor, we can categorize faulty and healthy signals.

The study is limited to investigating the mechanical faults of the DC servomotor, which can be considered a disadvantage. The drawback is recommended as a future work by involving armature and other electrical faults in this approach.

7. Conclusions

1. The proposed power consumption profile analysis approach succeeds to recognize the mechanical faults in the

gear-box of a DC servomotor via examining the mean level of the power consumption pattern.

2. The analysis of identifying the frequencies of interest by computing nominal RPM indicates that the speed of the output shaft of the healthy and faulty datasets differs very little and is very close to the theoretical value of 50 RPM.

3. The extraction of the Power Spectral Density indicates that it is possible to categorize faulty and healthy signals by comparing faulty and healthy PSDs.

Acknowledgments

The authors gratefully acknowledge the Department of Chemical Engineering and Petroleum Industries, Al-Mustaqbal University College-Babil-Iraq for the support.

References

- Gayatri Sarman, K. V. S. H., Madhu, T., Mallikharjuna Prasad, A. (2020). Prognosis of Inter-turn and Hall Sensor Faults of Brushless DC Motor Using ANFIS with Particle Swarm Optimization. *Journal of Advanced Research in Dynamical and Control Systems*, 12 (SP3), 1281–1292. doi: <https://doi.org/10.5373/jardcs/v12sp3/20201377>
- Kudelina, K., Asad, B., Vaimann, T., Belahcen, A., Rassölkin, A., Kallaste, A., Lukichev, D. V. (2020). Bearing Fault Analysis of BLDC Motor for Electric Scooter Application. *Designs*, 4 (4), 42. doi: <https://doi.org/10.3390/designs4040042>
- Munikoti, S., Das, L., Natarajan, B., Srinivasan, B. (2019). Data-Driven Approaches for Diagnosis of Incipient Faults in DC Motors. *IEEE Transactions on Industrial Informatics*, 15 (9), 5299–5308. doi: <https://doi.org/10.1109/tii.2019.2895132>
- Nandi, S., Toliyat, H. A., Li, X. (2005). Condition Monitoring and Fault Diagnosis of Electrical Motors – A Review. *IEEE Transactions on Energy Conversion*, 20 (4), 719–729. doi: <https://doi.org/10.1109/tec.2005.847955>
- Shifat, T. A., Hur, J. W. (2020). An Effective Stator Fault Diagnosis Framework of BLDC Motor Based on Vibration and Current Signals. *IEEE Access*, 8, 106968–106981. doi: <https://doi.org/10.1109/access.2020.3000856>
- Shifat, T. A., Hur, J.-W. (2020). EEMD assisted supervised learning for the fault diagnosis of BLDC motor using vibration signal. *Journal of Mechanical Science and Technology*, 34 (10), 3981–3990. doi: <https://doi.org/10.1007/s12206-020-2208-7>
- Hur, J.-W., Shifat, T. A. (2020). Motor vibration analysis for the fault diagnosis in non-stationary operating conditions. *International Journal of Integrated Engineering*, 12 (3), 151–160. Available at: <https://publisher.uthm.edu.my/ojs/index.php/ijie/article/view/5342/3400>
- Sabry, A. H., Nordin, F. H., Sabry, A. H., Abidin Ab Kadir, M. Z. (2020). Fault Detection and Diagnosis of Industrial Robot Based on Power Consumption Modeling. *IEEE Transactions on Industrial Electronics*, 67 (9), 7929–7940. doi: <https://doi.org/10.1109/tie.2019.2931511>
- Zhang, J., Zhan, W., Ehsani, M. (2018). On-line diagnosis of inter-turn short circuit fault for DC brushed motor. *ISA Transactions*, 77, 179–187. doi: <https://doi.org/10.1016/j.isatra.2018.03.029>
- Lü, D. G., Li, S. (2020). Fault diagnosis and fault tolerant control technology of brushless DC motor. *Dianji Yu Kongzhi Xuebao/Electric Mach Control*, 24 (8), 58–66. doi: <https://doi.org/10.15938/j.emc.2020.08.008>
- He, X., Ju, Y., Liu, Y., Zhang, B. (2017). Cloud-Based Fault Tolerant Control for a DC Motor System. *Journal of Control Science and Engineering*, 2017, 1–10. doi: <https://doi.org/10.1155/2017/5670849>
- Wahab, A. A., Abdullah, N. F., Rasid, M. A. H. (2019). Commutator fault detection of brushed DC motor using thermal assessment. *IOP Conference Series: Materials Science and Engineering*, 469, 012057. doi: <https://doi.org/10.1088/1757-899x/469/1/012057>
- Winston, D. P., Saravanan, M. (2013). Single Parameter Fault Identification Technique for DC Motor through Wavelet Analysis and Fuzzy Logic. *Journal of Electrical Engineering and Technology*, 8 (5), 1049–1055. doi: <https://doi.org/10.5370/jeet.2013.8.5.1049>
- Sabry, A. H., W. Hasan, W. Z., Ab. Kadir, M. Z. A., Radzi, M. A. M., Shafie, S. (2018). Field data-based mathematical modeling by Bode equations and vector fitting algorithm for renewable energy applications. *PLOS ONE*, 13 (1), e0191478. doi: <https://doi.org/10.1371/journal.pone.0191478>